ISSN 0030-400X, Optics and Spectroscopy, 2023, Vol. 131, No. 6, pp. 409–414. © Pleiades Publishing, Ltd., 2023.
Russian Text © The Author(s), 2022, published in Optika i Spektroskopiya, 2022, Vol. 130, No. 1, pp. 59–64.
English Text © Ioffe Institute, 2023.

Terahertz Spectroscopy of Magnetoelectric $HoAl_3(BO_3)_4$

A. M. Kuzmenko[a,*], V. Yu. Ivanov[a], A. Yu. Tikhanovsky[a], A. G. Pimenov[b], A. M. Shuvaev[b], I. A. Gudim[c], and A. A. Mukhin[a,]**

[a] *Prokhorov Institute of General Physics, Russian Academy of Sciences, Moscow, 119991 Russia*
[b] *Institute of Solid State Physics, Vienna University of Technology, Vienna, 1040 Austria*
[c] *Kirensky Institute of Physics, Siberian Branch, Russian Academy of Sciences, Krasnoyarsk, 660036 Russia*
**e-mail: krolandin@gmail.com*
***e-mail: mukhin@ran.gpi.ru*

Received August 2, 2021; revised August 2, 2021; accepted August 16, 2021

Abstract—Experimental and theoretical study of submillimeter (terahertz) spectroscopic and magnetic properties of the rare-earth aluminum borate $HoAl_3(BO_3)_4$ were performed at temperatures 3–300K. In the transmittance spectra a number of resonance lines were detected at frequencies 2–35 cm^{-1} for different radiation polarizations. These modes were identified as transitions between the lower levels of the ground multiplet of the Ho^{3+} ion split by the crystal field, including both transitions from the ground state to the excited ones and transitions between the excited states. The established excitation conditions of the observed modes and the simulation of the spectra made it possible to separate the magnetic and electric dipole transitions and to determine the energies of the corresponding states, their symmetry, and the matrix elements of the transitions. Low-frequency lines that do not fit into the established picture of the electron states of Ho^{3+} were also found; these lines, apparently, correspond to the ions with the distorted by defects local symmetry of the crystal field.

Keywords: Terahertz spectroscopy, rare earth aluminum borates, multiferroics, electron transitions
DOI: 10.1134/S0030400X23020121

INTRODUCTION

Rare earth borates $RM_3(BO_3)_4$ (R = Y, La–Lu; M = Fe, Al, Cr) with a crystal structure of trigonal symmetry (space group *R*32) attracted a particular interest in recent years. This is facilitated both by significant progress in growing large high-quality single crystals [1], and by the various magnetic, magnetoelectric, optical and other physical properties of borates [2–12]. Ferroborates $RFe_3(BO_3)_4$ are multiferroics in which the magnetic ordering of iron ions results in electric polarization [2]. Magnetoelectric interactions also cause anomalies in the dielectric permeability, which can manifest themselves in significant (up to 300%) changes in its value, as in $SmFe_3(BO_3)_4$ [3]. Aluminium borates $RAl_3(BO_3)_4$ are interesting for their luminescent and nonlinear optical properties [9, 10], they have no magnetic ordering, and electric polarization occurs only when a magnetic field is applied. In particular, in $TmAl_3(BO_3)_4$ a strong quadratic magnetoelectric effect was found [11], it is comparable in magnitude to the effect observed in ferroborates [2]. In holmium aluminoborate $HoAl_3(BO_3)_4$, an unprecedented value of magnetic fieldinduced electric polarization ~3600 $\mu C/m^2$ was found for crystals in a field 70 kOe at a temperature of 3 K [12]. For all borates a strong dependence of magnetic, magnetoelectric, spectroscopic, and other properties on the type of R ion is observed. In the aluminum borate $HoAl_3(BO_3)_4$ studied in this paper, the nature of the temperature dependences of the magnetic susceptibility and induced polarization [12] also indicates the prevailed contribution of low-frequency states to the magnetic and magnetoelectric properties.

The objective of this paper is terahertz spectroscopic studies of electronic transitions in the ground multiplet $^5I_8$ of the Ho^{3+} ion of aluminum borate $HoAl_3(BO_3)_4$, which are expected to make the main contribution to the magnetic, magnetoelectric, and dielectric properties.

EXPERIMENT

Large (up to 5 mm) single crystals of holmium aluminoborate were grown by crystallization from a solution in a melt on a seed [1]. To directly observe electronic transitions between low-energy states of the Ho^{3+} ion in $HoAl_3(BO_3)_4$, a study was carried out using the method of quasi-optical submillimeter (terahertz) spectroscopy with backward-wave tubes as a radiation source [13]. This method makes it possible to

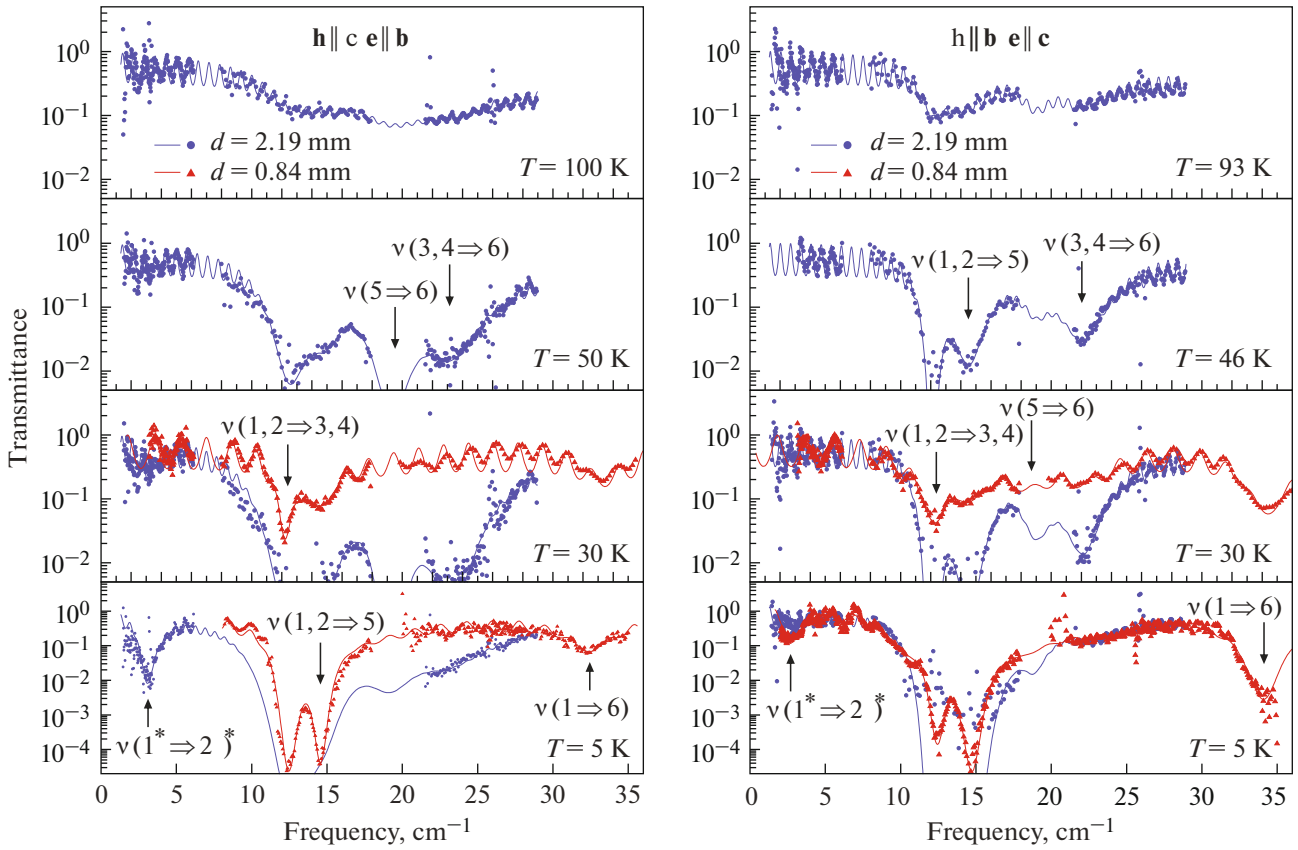

Fig. 1. Terahertz transmission spectra of a-section of $HoAl_3(BO_3)_4$ for radiation polarizations **h** ∥ **c**, **e** ∥ **b** (left column) and **h** ∥ **b**, **e** ∥ **c** (right column). Symbols are experimental data for different sample thicknesses: circles—d = 2.19 mm, triangles—d = 0.84 mm. Lines—theory.

monitor the polarization of radiation to determine the conditions for the transitions excitation. The transmission spectra of plane-parallel samples of a-section (the plane of the plate is perpendicular to **a** axis of the crystal) of $HoAl_3(BO_3)_4$ single crystal in the frequency range of 2–35 cm^{-1} were measured. Examples of spectra are shown in Fig. 1. Against the background of characteristic oscillations caused by interference in the plane-parallel sample, a complex pattern of the resonant absorption lines was observed in the sample as the temperature decreased. The frequencies of the resonance lines do not depend on temperature, while the intensities and widths of the lines change strongly with temperature. Since the intensity of some lines strongly increased with temperature decreasing, the transmission became lower than the level possible for detection, and thinner samples were prepared and measured. The spectra for different sample thicknesses were subsequently described in a consistent manner.

For most lines the intensity increases with temperature decreasing, while the intensity of the lines 3, 4 ⇒ 6 and 5 ⇒ 6 (Fig. 1) has a maximum and decreases with further temperature decreasing. This behavior indicates that the lines whose intensity increases with temperature decreasing correspond to transitions from the ground state to the excited levels, while the lines whose intensity temperature dependence has a maximum are determined by transitions between the excited levels.

ANALYSIS AND DISCUSSION OF EXPERIMENTAL RESULTS

Since in holmium aluminoborate there is no ordering in the magnetic subsystem of rare-earth ions up to 2 K, then there are no collective spin modes, and it is natural to identify the observed lines with magnetic and electric dipole electronic transitions inside the ground multiplet $^5I_8$ of the Ho^{3+} ion split by the crystal field. To obtain detailed information about the transitions, the obtained spectra were modeled (lines in Fig. 1) using the Fresnel formulas for plane-parallel layer, taking into account the contributions of the corresponding electronic transitions to the dispersion of the dielectric ε* and magnetic μ* permeabilities:

$$\varepsilon^*(\nu) = \varepsilon'(\nu) + i\varepsilon''(\nu) = \varepsilon_\infty + \sum_k \frac{\Delta\varepsilon_k \nu_k^2}{(\nu_k^2 - \nu^2) + i\nu_k\gamma_k}, \quad (1)$$

Table 1. Selection rules for transitions between symmetry states $\Gamma = E, A_1, A_2$ in crystal field of symmetry D_3 in non-Kramers ion Ho^{3+}. The components of the electric **d** and magnetic **μ** dipole moments are indicated, the off-diagonal matrix elements of which are nonzero, dash—transitions are forbidden

Γ	E	A_1	A_2
E	$d_{x,y,z}, \mu_{x,y,z}$	$d_{x,y}, \mu_{x,y}$	$d_{x,y}, \mu_{x,y}$
A_1	$d_{x,y}, \mu_{x,y}$	–	d_z, μ_z
A_2	$d_{x,y}, \mu_{x,y}$	d_z, μ_z	–

$$\mu^*(\nu) = \mu'(\nu) + i\mu''(\nu) = 1 + \sum_k \frac{\Delta\mu_k \nu_k^2}{(\nu_k^2 - \nu^2) + i\nu_k\gamma_k}, \quad (2)$$

where ν_k are resonant frequencies, $\Delta\mu_k$ and $\Delta\varepsilon_k$ are contributions to the magnetic and dielectric permeability (intensities) and γ_k are linewidths of the corresponding kth electronic transition (oscillator), and ε_∞ is high-frequency dielectric permeability.

The pattern of $HoAl_3(BO_3)_4$ absorption lines turned out to be quite rich (Fig. 1). The ground multiplet $^5I_8$ of the non-Kramers ion Ho^{3+} in the crystal field of symmetry D_3 splits into singlets (A_1 and A_2) and doublets (E), the selection rules between which for magnetic-electric dipole transitions are given in the Table 1 [8].

To analyze the resulting spectrum, the results of the paper [14] were used, where the level structure of the ground multiplet of the Ho^{3+} ion in the diluted system $Ho_{0.01}Y_{0.99}Al_3(BO_3)_4$ was determined. Based on these data, initial assumptions were made about the positions and symmetry of the levels of the rare-earth ion

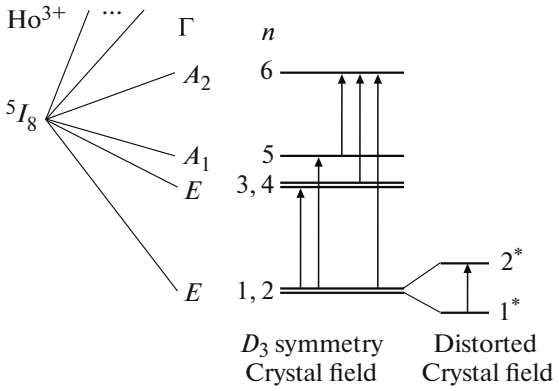

Fig. 2. Diagram of the lower electronic states of the ground multiplet of the Ho^{3+} ion in $HoAl_3(BO_3)_4$ crystal. The arrows indicate the transitions observed in the spectra. On the right is the diagram of additional splitting of the ground state due to possible distortions of the local symmetry of the crystal field.

Table 2. Identification of the observed resonant modes by excitation conditions (magnetic or electric dipole). In first column—the symbol of the resonance line, which represents the levels of the corresponding transitions; in the second column—frequencies of the resonant lines; further—contributions to the line intensity for different radiation polarizations

$n_i \Rightarrow n_j$	$\nu(n_i \Rightarrow n_j)$, cm^{-1}	a-cut		c-cut
		h ∥ c, e ∥ b	**h ∥ b, e ∥ c**	**h ∥ a, e ∥ b**
1, 2 ⇒ 3, 4	12.3	$\Delta\mu_c, \Delta\varepsilon_b$	$\Delta\mu_b, \Delta\varepsilon_c$	$\Delta\mu_a, \Delta\varepsilon_b$
1, 2 ⇒ 5	14.5	$\Delta\varepsilon_b$	$\Delta\mu_b$	$\Delta\mu_a, \Delta\varepsilon_b$
5 ⇒ 6	18.9	$\Delta\mu_c$	$\Delta\varepsilon_c$	–
3, 4 ⇒ 6	21.2	$\Delta\varepsilon_b$	$\Delta\mu_b$	$\Delta\mu_a, \Delta\varepsilon_b$
1, 2 ⇒ 6	34	$\Delta\varepsilon_b$	$\Delta\mu_b$	$\Delta\mu_a, \Delta\varepsilon_b$

in $HoAl_3(BO_3)_4$ (Fig. 2). The levels of two lower doublets E and two singlets A_1 and A_2 fall into the frequency range studied by us, and the energy of the next excited level is 126 cm^{-1}. In paper [15] the energy levels and crystal field parameters from paper [14] were used to describe the magnetic and magnetoelectric properties of undiluted $HoAl_3(BO_3)_4$, which showed their good agreement with the parameters of the concentrated composition. Thus, six of the 17 states of multiplet $^5I_8$ will be considered, transitions between which were observed in the studied terahertz spectra.

The Table 2 lists the excitation conditions for transitions between different states, considering the selection rules (Table 1), and gives the designations of the observed modes: levels are shown, transitions between which contribute to the corresponding resonant line. To identify the conditions for modes excitation, their contributions to ε* or μ* for different orientations of the alternating magnetic **h** and electric **e** fields with respect to the crystallographic axes are also given.

Thus, most of the lines (except 1, 2 ⇒ 3, 4) in a-section sample can be unambiguously identified as magnetic or electric dipole in each of the polarizations. The corresponding transition frequencies obtained from the simulation of the observed resonant lines in the transmission spectra made it possible to determine the energies of the considered states: $E_{1,2} = 0\ cm^{-1}$, $E_{3,4} = 12.3\ cm^{-1}$, $E_5 = 14.5\ cm^{-1}$, $E_6 \approx 34\ cm^{-1}$, which agrees well with the results of paper [14]. Nonzero matrix elements of magnetic dipole transitions expressed in Bohr magnetons (μ_B) are given in the Table 3. The parameters of the resonance lines (frequencies and contributions) observed in $HoAl_3(BO_3)_4$ are shown in Fig. 3. Figures 3b, 3e describes the temperature dependences of the contributions to the magnetic permeability μ* from magnetic dipole transi-

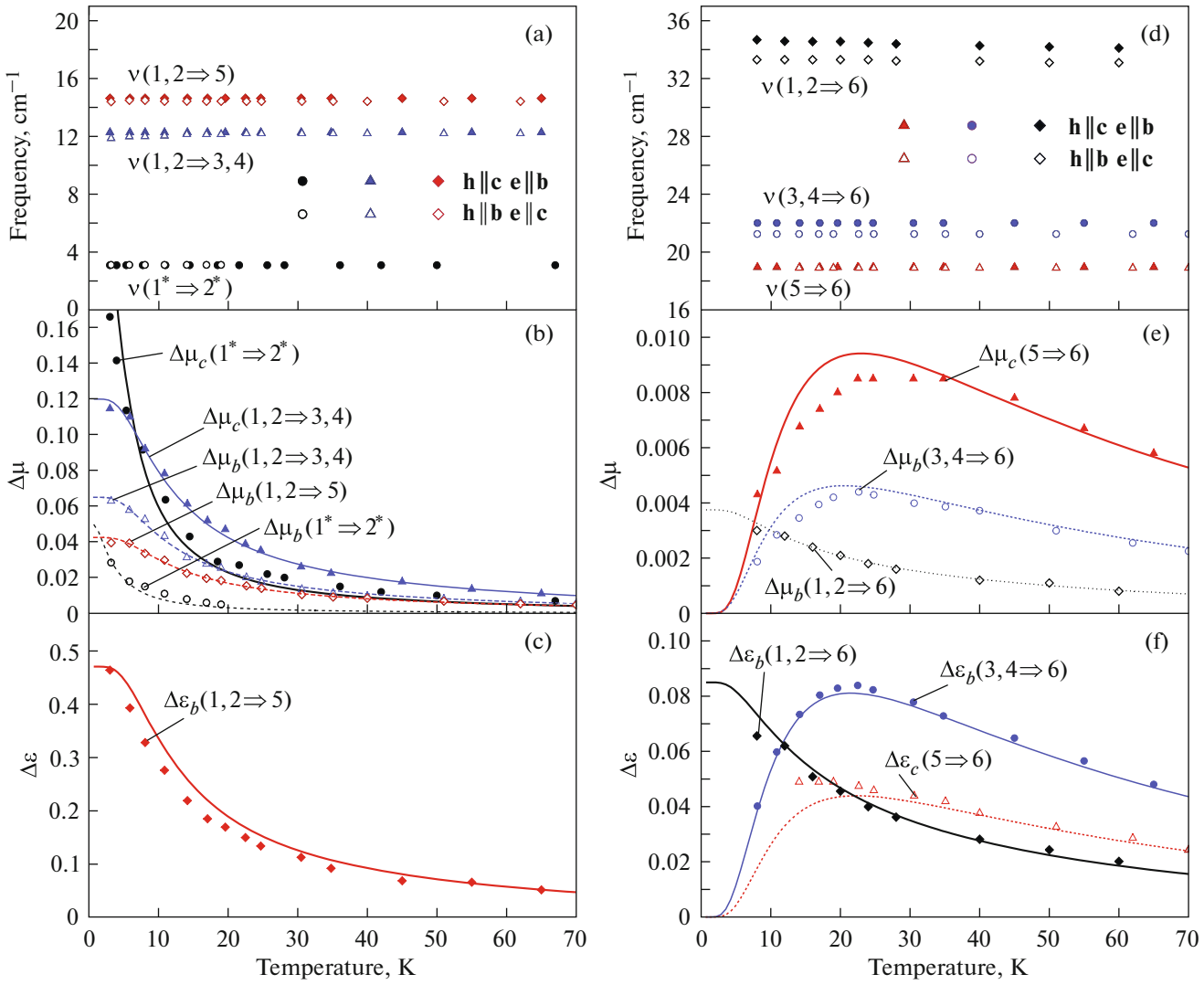

Fig. 3. Temperature dependences of the resonance mode parameters: frequencies (a, d), contributions to the magnetic (b, e) and dielectric (c, f) permeability. Symbols—experiment, lines—theory.

tions. For the contribution to the magnetic permeability of transition between states i and j, we have

$$\Delta\mu_{i,j}^{b,c} = 4\pi\rho\frac{N_A}{M_{\text{mol}}}\frac{2(\mu_{ij}^{b,c})^2}{Z(E_j - E_i)}\left(e^{-\frac{E_i}{k_BT}} - e^{-\frac{E_j}{k_BT}}\right), \quad (3)$$

where N_A is Avogadro number; M_{mol} is molar mass; Z is partition function; $\mu_{ij}^{b,c}$ is modulus of transition matrix element (Table 3) for the corresponding orientation of the alternating magnetic field $\mathbf{h} \| \mathbf{b}$ or $\mathbf{h} \| \mathbf{c}$; $E_{i,j}$ are energies of the initial and final states of the transition. Note that expression (3) gives the contribution of the observed resonant line to the magnetic permeability for transitions between singlets (5 ⇒ 6) only. To calculate the line contributions determined by states including degenerate doublets, it is necessary to sum the contributions of components $\Delta\mu_{ij}^{b,c}$ of the doublet transitions. For example, the contribution of transition 1, 2 ⇒ 6 $\Delta\mu_b(1, 2 \Rightarrow 6) = \Delta\mu_{16}^b + \Delta\mu_{26}^b = 2\Delta\mu_{16}^b$.

Similar dependences describe the contributions to the dielectric permeability of electric dipole transitions (Figs. 3c, 3f):

$$\Delta\varepsilon_{i,j}^{b,c} = 4\pi\rho\frac{N_A}{M_{\text{mol}}}\frac{2(d_{ij}^{b,c})^2}{Z(E_j - E_i)}\left(e^{-\frac{E_i}{k_BT}} - e^{-\frac{E_j}{k_BT}}\right), \quad (4)$$

where $d_{ij}^{b,c}$ is matrix element of the transition. From the descriptions of the temperature dependences of the contributions of electroactive modes (Figs. 3c, 3f), the following values of matrix elements (electric dipole

Table 3. Moduli of matrix elements for magnetic dipole transitions (in Bohr magnetons) between lower states of symmetry $\Gamma = E, A_1, A_2$ of ground multiplet of the Ho^{3+} ion found from the experimental values of the magnetic contributions. Dash—value not determined

(a) $\mu^{a,\,b}$								(b) μ^{c}							
n		1	2	3	4	5	6	n		1	2	3	4	5	6
	Γ	E	E	E	E	A_2	A_1		Γ	E	E	E	E	A_2	A_1
1	E	0	0	0	≤3.6	3.2	1.5	1	E	–	0	≤4.9	0	0	0
2	E	0	0	≤3.6	0	3.2	1.5	2	E	0	–	0	≤4.9	0	0
3	E	0	≤3.6	0	0	–	3.0	3	E	≤4.9	0	–	0	0	0
4	E	≤3.6	0	0	0	–	3.0	4	E	0	≤4.9	0	–	0	0
5	A_2	3.2	3.2	–	–	0	0	5	A_2	0	0	0	0	0	6.1
	A_1	1.5	1.5	3.0	3.0	0	0	6	A_1	0	0	0	0	6.1	0

moments in Debye) are obtained: $d^b_{15} = d^b_{25} = 0.1$ D, $d^b_{16} = d^b_{26} = 0.06$ D, $d^b_{36} = d^b_{46} = 0.11$ D, $d^c_{56} = 0.12$ D.

In the transmission spectra, in addition to the identified absorption lines, a low-frequency mode $1^* \Rightarrow 2^*$ was observed. Its contribution in different polarizations increases up to low temperatures, which indicates that it corresponds to transitions from the ground state. Thus, it cannot be interpreted as a transition between the excited levels 3, $4 \Rightarrow 5$. For certainty, when describing the intensity of this line, it was considered as magnetic dipole line and was described using the expression (3) by the contribution to the magnetic permeability (Fig. 3b). For this description, the values of the matrix elements $\mu^b_{1^*2^*} = 2.1\ \mu$B, $\mu^c_{1^*2^*} = 4.2\ \mu$B were obtained. This mode may also contain the contribution of electric dipole transitions. A possible reason for this mode appearance could be transitions between the components of the ground doublet split due to local distortions of their symmetry D_3 for a number of positions of rare-earth ions (see the right side of Fig. 2). No noticeable signs of such splitting were found for the above laying modes, which may indicate a small number of distorted positions. This effect can be due to Bi impurities similarly to that found earlier in $TmAl_3(BO_3)_4$ [16] and $YbAl_3(BO_3)_4$ [17]. Another reason for lowering the local D_3 symmetry of the Ho^{3+} ions could be Jahn–Teller distortions of the crystalline environment of the rare-earth ion, which remove the degeneracy of the two states of the lower doublet. This could also be accompanied by cooperative distortions of the lattice, which require further studies. The extent of these two mechanisms coexistence and influence each other also requires further study.

For the high-frequency modes ($1.2 \Rightarrow 6$), ($3.4 \Rightarrow 6$) some frequency mismatch was observed in the polarizations $\mathbf{h} \parallel \mathbf{c}$, $\mathbf{e} \parallel \mathbf{b}$ and $\mathbf{h} \parallel \mathbf{b}$, $\mathbf{e} \parallel \mathbf{c}$ (Fig. 3d). This may be the result of additional distortion of the line shape due to optical activity (rotation of the plane of polarization and changes in the ellipticity of the passed radiation), which manifests itself in other aluminium borates, in particular in $YbAl_3(BO_3)_4$ [18].

Based on the theoretical description of the identified magnetic lines, the moduli of the off-diagonal matrix elements were determined (Table 3). In view of the uncertainty in the excitation conditions of mode 1, $2 \Rightarrow 3$, 4, its intensity is described by the magnetic dipole contribution to the magnetic permeability (2). Therefore, for the values of off-diagonal matrix elements of transitions between doublets 1, $2 \Rightarrow 3$, 4 (Table 3) the upper limit of their values is actually defined. It is possible that part of the intensity of the 1, $2 \Rightarrow 3$, 4 transition line may also be due to the electric dipole transition.

Figure 4 shows the temperature dependences of the magnetic susceptibility of $HoAl_3(BO_3)_4$, the lines are the total contribution of all observed magnetic dipole transitions, it is assumed that 1, $2 \Rightarrow 3$, 4 transitions only contribute to the magnetization. This result confirms the prevailing contribution to the magnetization of the considered lower electronic states Ho^{3+}. The main doublet $1 \Rightarrow 2$ in undistorted positions could give an additional contribution to the magnetization along **c** axis due to diagonal matrix elements, then in the direction perpendicular to **c** the undistorted positions should not give additional contribution to the magnetization, which agrees with the description of the magnetic susceptibility (Fig. 4).

CONCLUSION

Using terahertz spectroscopy in the frequency range of 2–35 cm^{-1}, direct observation of electronic transitions between the lower levels of the ground multiplet of the Ho^{3+} ion in the aluminum borate $HoAl_3(BO_3)_4$ was performed. The resonant lines found in the transmission spectra are identified as electronic transitions excited by the electric or magnetic component of the alternating radiation field.

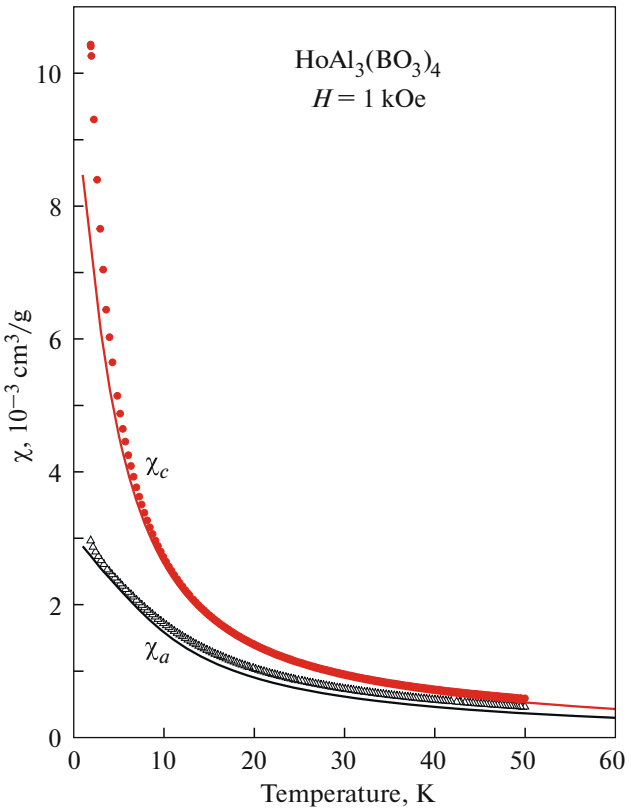

Fig. 4. Magnetic susceptibility of aluminoborate $HoAl_3(BO_3)_4$ along (χ_c) and perpendicular (χ_a) to the axis **c** of the crystal vs temperature. Symbols—experiment, lines—calculation of the sum of contributions to the magnetic susceptibility from all observed low-frequency transitions.

From the theoretical description of the temperature dependences of the resonance line parameters, both the positions of the energy levels and the matrix elements of the transitions are reconstructed. In addition to the lines corresponding to the transitions between the levels Ho^{3+} in the highly symmetrical crystal field of aluminoborate, the additional low-frequency lines were found, which presumably correspond to rare earth positions in the crystal field distorted by local defects. It was determined that the magnetization of $HoAl_3(BO_3)_4$ at low temperatures is mainly determined by the observed transitions.

FUNDING

This study was partially financially supported by the Russian Science Foundation (project 16-12-10531).

CONFLICT OF INTEREST

The authors of this work declare that they have no conflict of interest.

REFERENCES

1. V. L. Temerov, A. E. Sokolov, A. L. Sukhachev, A. F. Bovina, Edel'man, A. V. Malakhovskii, Crystallogr. Rep. **53**, 1157 (2008).
2. M. Kadomtseva, Yu. F. Popov, G. P. Vorob'ev, A. P. Pyatakov, S. S. Krotov, K. I. Kamilov, V. Yu. Ivanov, A. A. Mukhin, A. K. Zvezdin, A. M. Kuzmenko, L. N. Bezmaternykh, I. A. Gudim, V. L. Temerov, Fizika nizkikh temperatur **36** (6), 640 (2010).
3. A. A. Mukhin, G. P. Vorob'ev, V. Yu. Ivanov, A. M. Kadomtseva, A. S. Narizhnaya, A. M. Kuzmenko, Yu. F. Popov, L. N. Bezmaternykh, I. A. Gudim, JETP Lett. **93** (5), 275 (2011).
4. S. A. Klimin, D. Fausti, A. Meetsma, L. N. Bezmaternykh, P. H. M. van Loosdrecht, T. T. M. Palstra, Acta Crystallogr., Sect. B: Struct. Sci. **61**, 481 (2005).
5. M. N. Popova, E. P. Chukalina, K. N. Boldyrev, T. N. Stanislavchuk, B. Z. Malkin, I. A. Gudim, Phys. Rev. B **95**, 125131 (2017).
6. M. N. Popova, B. Z. Malkin, K. N. Boldyrev, T. N. Stanislavchuk, D. A. Erofeev, V. L. Temerov, I. A. Gudim, Phys. Rev. B **94**, 184418 (2016).
7. M. N. Popova, T. N. Stanislavchuk, B. Z. Malkin, L. N. Bezmaternykh, Phys. Rev. B **80**, 195101 (2009).
8. M. N. Popova, E. P. Chukalina, D. A. Erofeev, I. A. Gudim, I. V. Golosovsky, A. Gukasov, A. A. Mukhin, B. Z. Malkin, Phys. Rev. B **103**, 094411 (2021).
9. A. V. Malakhovskii, I. S. Edelman, A. E. Sokolov, V. L. Temerov, S. L. Gnatchenko, I. S. Kachur, V. G. Piryatinskaya, Phys. Lett. A **371**, 254 (2007).
10. A. V. Malakhovskii, U. V. Valiev, I. S. Edelman, A. E. Sokolov, I. Yu. Chesnokov, I. A. Gudim, Optical Materials **32**, 1017 (2010).
11. R. P. Chaudhury, F. Yen, B. Lorenz, Y. Y. Sun, L. N. Bezmaternykh, V. L. Temerov, C. W. Chu, Phys. Rev. B **81**, 220402(R) (2010).
12. K.-C. Liang, R. P. Chaudhury, B. Lorenz, Y. Y. Sun, L. N. Bezmaternykh, V. L. Temerov, C. W. Chu, Phys. Rev. B **83**, 180417(R) (2011).
13. A. A. Volkov, Yu. G. Goncharov, G. V. Kozlov, S. P. Lebedev, A. M. Prokhorov, Infrared Phys. **25**, 369 (1985).
14. A. Baraldi, R. Capelletti, M. Mazzera, N. Magnani, I. Földvari, E. Beregi, Phys. Rev. B **76**, 165130 (2007).
15. N. V. Kostyuchenko, A. I. Popov, A. K. Zvezdin, Solid State Phenomena **215**, 95 (2014).
16. A. M. Kuzmenko, A. A. Mukhin, V. Yu. Ivanov, G. A. Komandin, A. Shuvaev, A. Pimenov, V. Dziom, L. N. Bezmaternykh, I. A. Gudim, Phys. Rev. B **94**, 174419 (2016).
17. K. N. Boldyrev, M. N. Popova, M. Bettinelli, V. L. Temerov, I. A. Gudim, L. N. Bezmaternykh, P. Loiseau, G. Aka, N. I. Leonyuk, Optical Materials **34**, 1885 (2012).
18. A. M. Kuzmenko, V. Dziom, A. Shuvaev, A. Pimenov, D. Szaller, A. A. Mukhin, V. Yu. Ivanov, A. Pimenov, Phys. Rev. B **99**, 224417 (2019).